autopsied brains of four MS patients and nine non-MS subjects. All four MS cases were clinically diagnosed as chronic progressive MS, composed of three cases of secondary progressive MS (SPMS) and one case of primary progressive MS (PPMS). Non-MS cases included a previously reported case of neuromyelitis optica (NMO),[23] four neurologically normal control (NC) subjects and four patients with cerebral infarction. Their clinical characteristics are shown in Table S1. Autopsies were carried out at the National Center Hospital, National Center of Neurology and Psychiatry (NCNP), Kohnodai Hospital, National Center for Global Health and Medicine (NCGM) or the Nishitaga National Hospital. The comprehensive examination by three established neuropathologists (KA, YS, TI) validated the pathological diagnosis. Written informed consent was obtained from all the cases. The ethics committee of the corresponding institutions approved the present study.

Immunohistochemistry

Immunohistochemical studies were carried out according to the methods described previously.[24] In brief, after deparaffination, tissue sections were heated in 10 mM citrate sodium buffer, pH 6.0 by autoclave at 110°C for 15 min in a temperature-controlled pressure chamber (Biocare Medical, Concord, CA, USA). They were treated at room temperature for 15 min with 3% hydrogen peroxide-containing methanol to block the endogenous peroxidase activity. The tissue sections were then incubated with phosphate-buffered saline (PBS) containing 10% normal goat serum at room temperature for 15 min to block non-specific staining. They were incubated in a moist chamber at 4°C overnight with a rabbit antibody against the peptide mapping to the N-terminus of the human NLRP3 protein (1:300; HPA012878; Sigma, St. Louis, MO, USA), a rabbit antibody against a mixture of the peptides mapping at amino acid residues 31–46 and 94–110 of the human ASC protein (1:100; ab113225; Abcam, Cambridge, England), a rabbit antibody against the C-terminal peptide of the human CASP1 p10 protein (1:500; sc-515; Santa Cruz Biotechnology, Santa Cruz, CA, USA) and a rabbit antibody against the peptide mapping at amino acid residues of 117–269 of the human IL-1B protein (1:50; sc-7884; Santa Cruz Biotechnology). After washing with PBS, the tissue sections were labeled at room temperature for 30 min with horseradish peroxidase (HRP)-conjugated secondary antibodies (Nichirei, Tokyo, Japan), followed by incubation with diaminobenzidine tetrahydrochloride (DAB) substrate (Vector, Burlingame, CA, USA). They were processed for a counterstain with hematoxylin. Negative controls underwent all the steps except for exposure to primary antibody. We classified chronic demyelinating lesions of MS into either "chronic active", defined as a lesion with a hypocellular center and a hypercellular rim, or "chronic inactive", defined as a hypocellular lesion.[25]

For double labeling, tissue sections were initially stained with anti-NLRP3 antibody HPA012878. After autoclaving, they were labeled with prediluted mouse antibodies against GFAP (GA5; Nichirei) or CD68 (KP1; Dako, Tokyo, Japan), followed by incubation with alkaline phosphatase (AP)-conjugated secondary antibodies (Nichirei) and colorized with a Warp Red chromogen (Biocare Medical, Concord, CA, USA).

Reverse transcription polymerase chain reaction analysis

Total RNA was isolated from a panel of human cell lines described previously.[26] Total RNA of the human frontal cerebral cortex (Clontech, Mountain View, CA, USA) was also processed in parallel for reverse transcription polymerase chain reaction (RT–PCR). DNase-treated total RNA was processed for cDNA synthesis using oligo(dT)$_{12-18}$ primers and SuperScript II reverse transcriptase (Invitrogen, Carlsbad, CA, USA). Then, cDNA was amplified by PCR using HotStar Taq DNA polymerase (Qiagen, Valencia, CA, USA), and the following panel of sense and antisense primer sets: 5′ agtgctgaaacagcagagctgcct3′ and 5′ccgtttccactcctaccaagaagg3′ for a 151 bp product of *NLRP3*; 5′ agtttcacaccagcctggaactgg3′ and 5′ggatgatttggtgggattgccagg3′ for a 153 bp product of *ASC*; 5′tggagacatcccacaatgggctct3′ and 5′cactctttcagtggtgggcatctg3′ for an 159 bp product of *CASP1*; 5′tgcccagttccccaactggtacat3′ and 5′ aggactctctgggtacagctctct3′ for a 145 bp product of *IL-1B*; and 5′ccatgttcgtcatgggtgtgaacca3′ and 5′gccagtagaggcagggatgatgttc3′ for a 251 bp product of the *glyceraldehyde-3-phosphate dehydrogenase* (*G3PDH*) gene that serves as an internal control. The amplification program consisted of an initial denaturing step at 95°C for 15 min, followed by a denaturing step at 94°C for 1 min, an annealing step at 60°C for 40 s and an extension step at 72.9°C for 50 s for 35 cycles, except for G3PDH amplified for 28 cycles.

Transient expression of NLRP3, ASC, and CASP1 in HEK293 cells

Open reading frames (ORF) of the human *NLRP3* gene (GenBank NM_004895), the human *ASC* gene (GenBank NM_013258) and the human *CASP1* gene (GenBank NM_033292) were amplified by PCR using PfuTurbo DNA polymerase (Stratagene, La Jolla, CA, USA), and the following sense and antisense primer sets: 5'gcaagcacccgctgcaagctggcc3' and 5'ctaccaagaaggctcaaagacgac3' for *NLRP3*, 5' gggcgcg cgcgcgacgccatcctg3' and 5'tcagctccgctccaggtcctccac3' for *ASC*, and 5' gccgacaaggtcctgaaggagaag3' and 5' ttaatgtcctgggaagaggtagaa3' for *CASP1*. Then, they were cloned in a mammalian expression vector named pcDNA4/HisMax-TOPO (Invitrogen). Then, the vectors were transfected into HEK293 cells by using Lipofectamine 2000 reagent (Invitrogen). At 24 h after transfection, the cells were processed for western blot analysis.

Western blot analysis

To prepare the total protein extract, the cells were homogenized in RIPA lysis buffer (Sigma) and a cocktail of protease inhibitors, followed by centrifugation at 13 400 rpm for 5 min at room temperature. The supernatant was separated on a 12% sodium dodecylsulfate polyacrylamide gel electrophoresis gel. After gel electrophoresis, the protein was transferred onto nitrocellulose membranes, and immunolabeled at room temperature overnight with the aforementioned primary antibodies. Then, the membranes were incubated at room temperature for 30 min with HRP-conjugated secondary antibodies (Santa Cruz Biotechnology). The specific reaction was visualized by using a chemiluminescent substrate (Pierce, Rockford, IL, USA). After the antibodies were stripped by incubating the membranes at 50°C for 30 min in a stripping buffer composed of 62.5 mM Tris-HCl, pH 6.7, 2% sodium dodecylsulfate and 100 mM 2-mercaptoethanol, the membranes were relabeled with a goat anti-heat shock protein HSP60 antibody (sc-1052; Santa Cruz Biotechnology) to assess an internal control for protein loading.

Results

Expression of NLRP3 inflammasome components in human neural cell lines

First, we studied NLRP3, ASC, CASP1 and IL-1B mRNA expression in a panel of human neural cell lines by RT–PCR. The complete set of NLRP3, ASC, CASP1 and IL-1B mRNA were expressed at variable levels in human cerebral (CBR) brain tissues, astrocytes (AS), neural progenitor (NP) cells, NTera2-deived differentiated neurons (NTera2N), T98G glioblastoma and HMO6 microglia, where the levels of G3PDH, a housekeeping gene, were almost constant (Fig. 1a–e; lanes 1, 3–5, 9, 10). When omitting the RT step, no PCR products were amplified (Fig. 1a–e; lane 2). The highest levels of NLRP3 and IL-1B were identified in NTera2N, whereas the highest levels of ASC and CASP1 were found in T98G. These results showed that the levels of the constitutive expression of NLRP3 inflammasome components are highly variable among distinct neural cell types.

Expression of NLRP3 inflammasome components in reactive astrocytes and perivascular macrophages in chronic active demyelinating lesions of MS, active necrotic lesions of NMO, and acute infarct lesions

Next, to verify the specificity of anti-NLRP3 antibody (HPA012878), anti-ASC antibody (ab113225) and

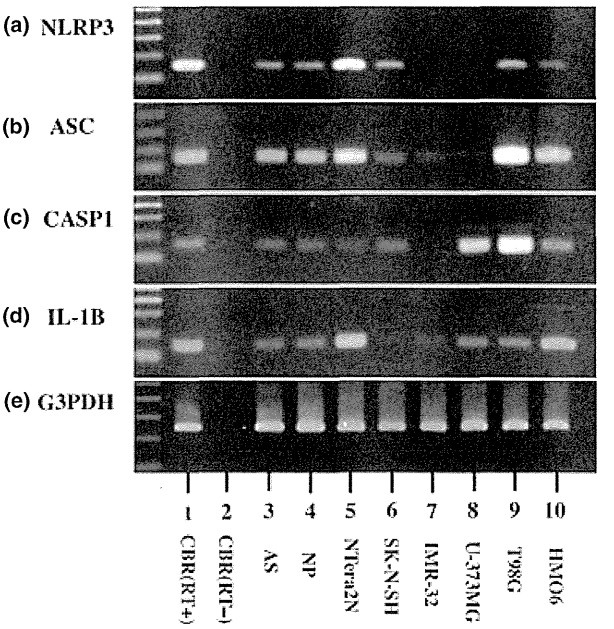

Figure 1 The expression of NLRP3 inflammasome components in human neural cell lines. The mRNA expression of (a) NLRP3, (b) ASC, (c) caspase-1 (CASP1), and (d) interleukin (IL)-1B, and (e) glyceraldehyde-3-phosphate dehydrogenase (G3PDH) was studied by reverse transcription (RT) polymerase chain reaction in human brain tissues and neural cell lines in culture. The lanes represent (1) cerebral (CBR) brain tissues with inclusion of RT step, (2) CBR without inclusion of RT-step, (3) astrocytes (AS), (4) neural progenitor (NP) cells, (5) NTera2-deived differentiated neurons (NTera2N), (6) SK-N-SH neuroblastoma, (7) IMR-32 neuroblastoma, (8) U-373MG astrocytoma, (9) T98G glioblastoma and (10) HMO6 microglia.

anti-CASP1 antibody (sc-515) utilized in the present study, the human *NLRP3*, *ASC* and *CASP1* genes cloned in the mammalian expression vector were expressed in HEK293 cells for western blot analysis. HPA012878, ab113225 and sc-515 reacted individually with the corresponding recombinant proteins of NLRP3, ASC or CASP1, but not with protein extract isolated from non-transfected cells (Fig. S1a–c). These results validated the specificity of the antibodies tested.

Then, we studied the expression of three components of NLRP3 inflammasome, along with IL-1B, in the cerebral cortex sections of four MS and nine non-MS cases by immunohistochemistry using the aforementioned antibodies. In the brains of neurologically normal control (NC) subjects, NLRP3 expression was restricted in a rare population (less than 0.01% of total cells) that represent a specified subset of ramified microglial cells often located in deep cortical layers and the white matter (Fig. S2a). All neurons, oligodendrocytes, astrocytes and the great majority of ramified microglia did not express discernible levels of NLRP3. In NC brains, ASC and CASP1 were undetectable except for a small subset (less than 0.1%) of ramified microglia (Fig. S2b,c). In contrast, IL-1B was expressed in many neurons with the location in the cytoplasm and in a small population (less than 1%) of ramified microglia (Fig. S2d).

Notably, numerous reactive astrocytes accumulating in chronic active demyelinating lesions of MS expressed intense immunoreactivities for NLRP3, ASC, CASP and IL-1B with the location in the cytoplasm (Fig. 2a–d, Fig. 3e). In contrast, the levels of expression of NLRP3, ASC, CASP, and IL-1B were much lower in reactive astrocytes and glial scars in chronic inactive lesions of MS. Furthermore, a large number of perivascular foamy macrophages expressed NLRP3, ASC, CASP and IL-1B at variable intensities in chronic active demyelinating lesions of MS (Fig. 3a–d,f). In contrast, the great majority of amoeboid and ramified microglia did not express NLRP3 in chronic active and inactive MS lesions (Fig. 3g). In the edge of active necrotic lesions of NMO, only hypertrophic reactive astrocytes and foamy macrophages intensely expressed the full set of NLRP3, ASC, CASP, and IL-1B (Fig. 4a–d). These results showed that reactive astrocytes and infiltrating macrophages engulfing tissue debris are the major cell types that express the complete set of NLRP3 components in active MS and NMO lesions.

In acute lesions of cerebral infarction, reactive astrocytes surrounding ischemic cores and foamy macrophages accumulating in necrotic lesions moderately expressed NLRP3, ASC, CASP, and IL-1B (Fig. 5a–d). In contrast, the levels of expression of NLRP3, ASC, CASP and IL-1B were low in any cell types in chronic gliotic lesions of cerebral infarction.

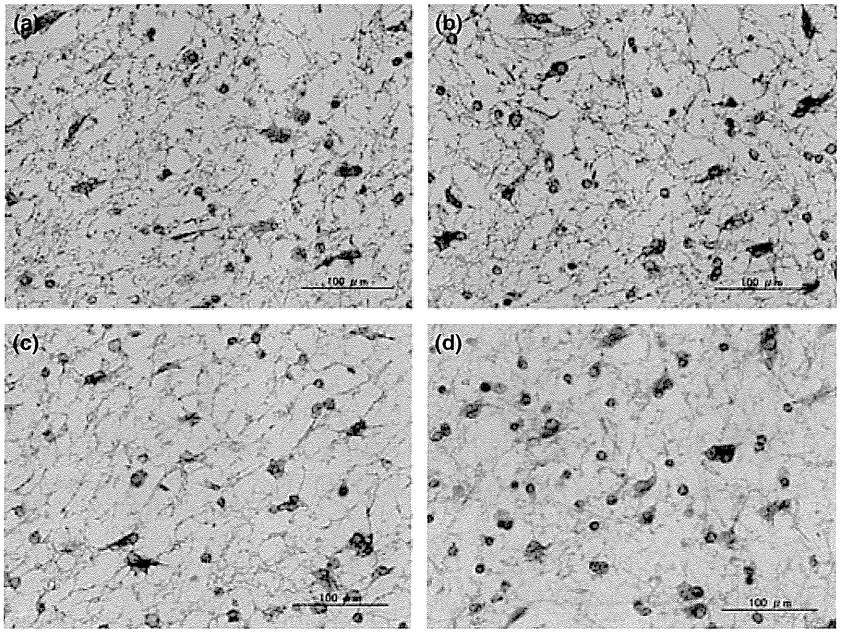

Figure 2 The expression of NLRP3 inflammasome components in reactive astrocytes in chronic active demyelinating lesions of multiple sclerosis. The expression of (a) NLRP3, (b) ASC, (c) caspase-1 and (d) interleukin-1B was studied in the serial sections of chronic active lesions of multiple sclerosis by immunohistochemistry. Reactive astrocytes intensely expressed all three components and interleukin -1B with the location of the cytoplasm.

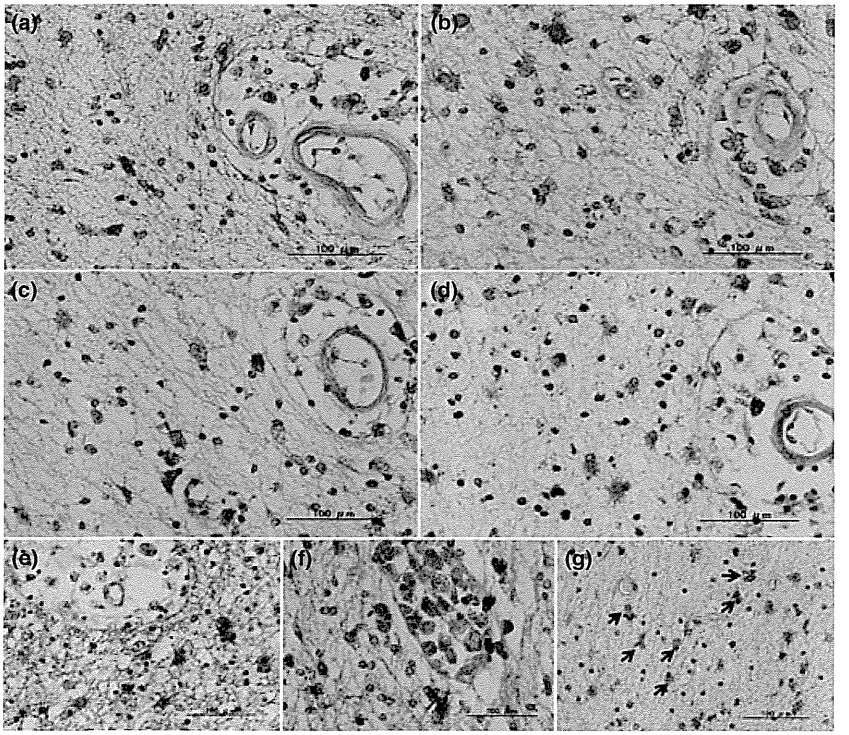

Figure 3 The expression of NLRP3 inflammasome components in perivascular macrophages in chronic active demyelinating lesions of multiple sclerosis. The expression of (a) NLRP3, (b) ASC, (c) caspase-1 and (d) interleukin-1B was studied in the serial sections of chronic active lesions of multiple sclerosis by immunohistochemistry. Perivascular macrophages expressed variable intensities of all three components and interleukin-1B in the cytoplasm. (e–g) Double immunolabeling of (e) NLRP3 (brown) and GFAP (red), (f) NLRP3 (brown) and CD68 (red), and (g) NLRP3 (brown) and CD68 (red). The arrows indicate CD68-positive NLRP3-negative ameboid microglial cells.

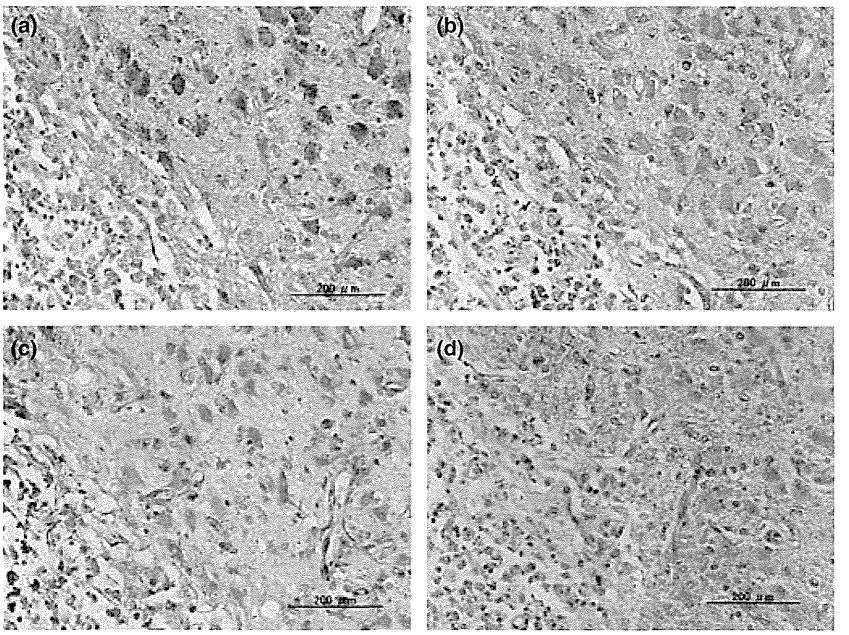

Figure 4 The expression of NLRP3 inflammasome components in reactive hypertrophic astrocytes and infiltrating macrophages in active necrotic lesions of neuromyelitis optica (NMO). The expression of (a) NLRP3, (b) ASC, (c) caspase-1 and (d) interleukin-1B was studied in the serial sections of active necrotic lesions of NMO by immunohistochemistry. Hypertrophic reactive astrocytes in the right upper half and foamy macrophages in the left lower half intensely expressed all three components and interleukin-1B with the location in the cytoplasm.

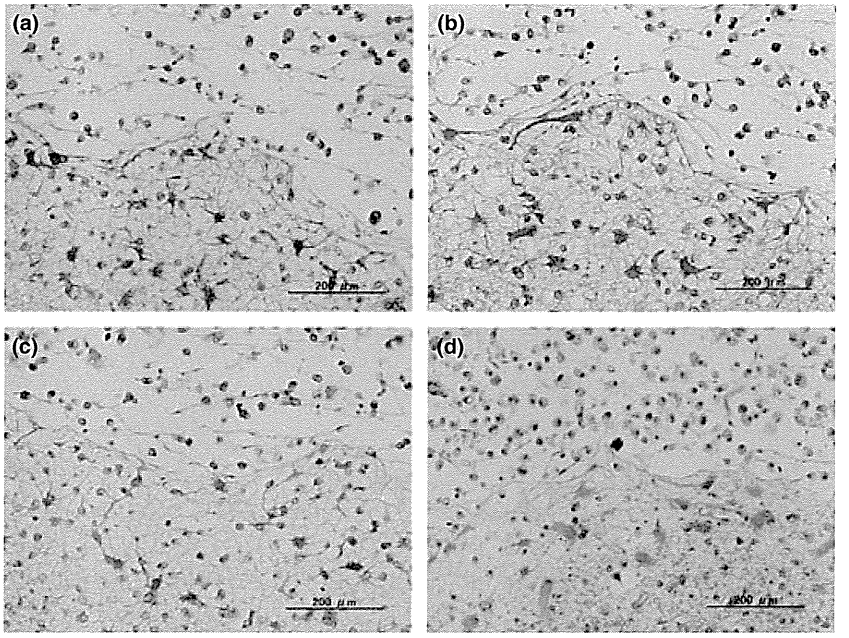

Figure 5 The expression of NLRP3 inflammasome components in reactive astrocytes and infiltrating macrophages in acute necrotic lesions of cerebral infarction. The expression of (a) NLRP3, (b) ASC, (c) caspase-1 and (d) interleukin-1B was studied in the serial sections of acute necrotic lesions of cerebral infarction by immunohistochemistry. Reactive astrocytes and foamy macrophages moderately expressed all three components and interleukin -1B with the location in the cytoplasm.

These results showed that NLRP3 inflammasome could be activated chiefly in astrocytes and macrophages under the condition of active destruction of brain tissues, regardless of the etiology, such as MS, NMO and cerebral infarction.

Discussion

By immunohistochemistry, we showed that reactive astrocytes and infiltrating foamy macrophages express the complete set of NLRP3 inflammasome components, such as NLRP3, ASC and CASP1, along with IL-1B in active demyelinating lesions of MS, active necrotic lesions of NMO and acute necrotic lesions of cerebral infarction. In contrast, the levels of expression of NLRP3, ASC, CASP, and IL-1B were substantially reduced in chronic inactive lesions of MS and chronic gliotic lesions of cerebral infarction, when compared with the expression levels in active demyelinating and necrotic lesions. We also found that the great majority of ramified and amoeboid microglia did not express NLRP3 in active and inactive MS lesions, and active NMO and infarct lesions. These results apparently contradict the observations of NLRP3 expression in HMO6 human microglial cells by RT–PCR, and the microglial expression of NLRP3 in a mouse model of AD.[15] However, a recent study elucidated NLRP3 inflammasome-independent mechanisms of IL-1B and IL-18 maturation in microglia.[27] Our observations suggest that NLRP3 inflammasome could be activated chiefly in astrocytes and macrophages under the condition of active destruction of brain tissues that potentially provides a danger signal, regardless of the etiology, such as MS, NMO and cerebral infarction. However, in the present study, the main limitation exists in non-quantitative analysis as a result of a small sample size analyzed by immunohistochemistry. To overcome this drawback, further examinations on large cohorts, including frozen brain tissues by western blot analysis, would be required.

Accumulating evidence shows that a diverse range of danger signals containing DAMP and PAMP effectively activate NLRP3 inflammasome.[1,2,7–10] Among the host-derived signals with DAMP, ATP is released extracellularly from damaged or dying cells after injury, infection and inflammation.[7,12] The activation of NLRP3 inflammasome in response to extracellular ATP is mediated by the purinergic receptor, P2X7, which recruits the pannexin-1 membrane channel.[7] Importantly, EAE is ameliorated by P2X7 receptor blockade.[28] Furthermore, the levels of P2X7 receptor expression are elevated in activated macrophages/microglia in the spinal cord of MS, suggesting the possible contribution of extracellular ATP to activation of NLRP3 in MS lesions.[29] Astrocytes also

express a P2X7 receptor and respond well to extracellular ATP.[30] It is worthy to note that acidic extracellular pH as a result of active destruction of brain tissues promotes NLRP3 inflammasome activation.[31]

A recent study showed that nanoparticles, such as 20 nm latex beads, could activate NLRP3 inflammasome in bone marrow-derived macrophages.[32] We could raise a possible scenario that brain tissue debris containing myelin degradation products of nanoparticle size, when taken up by phagocytosis, might serve as a danger signal for activation of NLRP3 inflammasome in infiltrating macrophages in active MS, NMO and infarct lesions. Furthermore, reactive astrocytes, as well as professional phagocytes, such as macrophages, microglia and dendritic cells, have a capacity to phagocytose damaged cells.[33] Mitochondrial injury generates excessive amounts of ROS in active MS lesions,[34] which potentially accelerates the assembly of NLRP3 inflammasome complex. NLRP3, translocated to mitochondria after activation of the inflammasome, regulates mitochondrial homeostasis.[35] Importantly, IFNβ inhibits activation of Rac1 through the SOCS1 signaling pathway, and reduces the generation of ROS.[36] Treatment with IFNβ is highly effective in a subtype of EAE whose development depends primarily on NLRP3 inflammasome, whereas it is ineffective in a distinct subtype of EAE independent of NLRP3 inflammasome activation induced by aggressive immunization.[36] In EAE, NLRP3 inflammasome promotes chemotactic migration of CD4+ T cells and antigen-presenting cells into the CNS, supporting a pro-inflammatory role of NLRP3 inflammasome.[37]

As clearance of damaged cellular constituents by locally accumulated phagocytes is a fundamental process to limit tissue damage, the present observations suggest the hypothesis that NLRP3 inflammasome expressed in reactive astrocytes and infiltrating macrophages plays a key role in not only amplification of inflammation, but also facilitation of tissue repair and regeneration by rapid and efficient production of IL-1B, serving as a potent growth factor for neural precursor cells, in MS, NMO and infarct lesions after acute tissue destruction.[38]

Acknowledgements

All autopsied brain samples were provided by Research Resource Network (RRN), Japan. This work was supported by grants from the JSPS KAKENHI (C22500322 and C25430054), the Ministry of Education, Culture, Sports, Science and Technology (MEXT), Japan. The authors declare no conflict of interest.

References

1. Schroder K, Tschopp J. The inflammasomes. *Cell.* 2010; **140**: 821–32.
2. Menu P, Vince JE. The NLRP3 inflammasome in health and disease: the good, the bad and the ugly. *Clin Exp Immunol.* 2011; **166**: 1–15.
3. Shi CS, Shenderov K, Huang NN, Kabat J, Abu-Asab M, Fitzgerald KA, et al. Activation of autophagy by inflammatory signals limits IL-1β production by targeting ubiquitinated inflammasomes for destruction. *Nat Immunol.* 2012; **13**: 255–63.
4. Wang H, Mao L, Meng G. The NLRP3 inflammasome activation in human or mouse cells, sensitivity causes puzzle. *Protein Cell.* 2013; **4**: 565–8.
5. Zhou R, Yazdi AS, Menu P, Tschopp J. A role for mitochondria in NLRP3 inflammasome activation. *Nature.* 2011; **469**: 221–5.
6. Shimada K, Crother TR, Karlin J, Dagvadorj J, Chiba N, Chen S, et al. Oxidized mitochondrial DNA activates the NLRP3 inflammasome during apoptosis. *Immunity.* 2012; **36**: 401–14.
7. Di Virgilio F. Liaisons dangereuses: $P2X_7$ and the inflammasome. *Trends Pharmacol Sci.* 2007; **28**: 465–72.
8. Halle A, Hornung V, Petzold GC, Stewart CR, Monks BG, Reinheckel T, et al. The NALP3 inflammasome is involved in the innate immune response to amyloid-β. *Nat Immunol.* 2008; **9**: 857–65.
9. Hafner-Bratkovič I, Benčina M, Fitzgerald KA, Golenbock D, Jerala R. NLRP3 inflammasome activation in macrophage cell lines by prion protein fibrils as the source of IL-1β and neuronal toxicity. *Cell Mol Life Sci.* 2012; **69**: 4215–28.
10. Codolo G, Plotegher N, Pozzobon T, Brucale M, Tessari I, Bubacco L, et al. Triggering of inflammasome by aggregated α-synuclein, an inflammatory response in synucleinopathies. *PLoS ONE.* 2013; **8**: e55375.
11. Sheedy FJ, Grebe A, Rayner KJ, Kalantari P, Ramkhelawon B, Carpenter SB, et al. CD36 coordinates NLRP3 inflammasome activation by facilitating intracellular nucleation of soluble ligands into particulate ligands in sterile inflammation. *Nat Immunol.* 2013; **14**: 812–20.
12. Hoegen T, Tremel N, Klein M, Angele B, Wagner H, Kirschning C, et al. The NLRP3 inflammasome contributes to brain injury in pneumococcal meningitis and is activated through ATP-dependent lysosomal cathepsin B release. *J Immunol.* 2011; **187**: 5440–51.
13. Kaushik DK, Gupta M, Kumawat KL, Basu A. NLRP3 inflammasome: key mediator of neuroinflammation in murine Japanese encephalitis. *PLoS ONE.* 2012; **7**: e32270.

14. Liu HD, Li W, Chen ZR, Hu YC, Zhang DD, Shen W, et al. Expression of the NLRP3 inflammasome in cerebral cortex after traumatic brain injury in a rat model. *Neurochem Res*. 2013; **38**: 2072–83.
15. Heneka MT, Kummer MP, Stutz A, Delekate A, Schwartz S, Vieira-Saecker A, et al. NLRP3 is activated in Alzheimer's disease and contributes to pathology in APP/PS1 mice. *Nature*. 2013; **493**: 674–8.
16. Lequerré T, Vittecoq O, Saugier-Veber P, Goldenberg A, Patoz P, Frébourg T, et al. A cryopyrin-associated periodic syndrome with joint destruction. *Rheumatology (Oxford)*. 2007; **46**: 709–14.
17. Compeyrot-Lacassagne S, Tran TA, Guillaume-Czitrom S, Marie I, Koné-Paut I. Brain multiple sclerosis-like lesions in a patient with Muckle-Wells syndrome. *Rheumatology (Oxford)*. 2009; **48**: 1618–9.
18. Ming X, Li W, Maeda Y, Blumberg B, Raval S, Cook SD, et al. Caspase-1 expression in multiple sclerosis plaques and cultured glial cells. *J Neurol Sci*. 2002; **197**: 9–18.
19. Jha S, Srivastava SY, Brickey WJ, Iocca H, Toews A, Morrison JP, et al. The inflammasome sensor, NLRP3, regulates CNS inflammation and demyelination via caspase-1 and interleukin-18. *J Neurosci*. 2010; **30**: 15811–20.
20. Gris D, Ye Z, Iocca HA, Wen H, Craven RR, Gris P, et al. NLRP3 plays a critical role in the development of experimental autoimmune encephalomyelitis by mediating Th1 and Th17 responses. *J Immunol*. 2010; **185**: 974–81.
21. Inoue M, Shinohara ML. The role of interferon-β in the treatment of multiple sclerosis and experimental autoimmune encephalomyelitis – in the perspective of inflammasomes. *Immunology*. 2013; **139**: 11–8.
22. Guarda G, Braun M, Staehli F, Tardivel A, Mattmann C, Förster I, et al. Type I interferon inhibits interleukin-1 production and inflammasome activation. *Immunity*. 2011; **34**: 213–23.
23. Satoh J, Obayashi S, Misawa T, Tabunoki H, Yamamura T, Arima K, et al. Neuromyelitis optica/Devic's disease: gene expression profiling of brain lesions. *Neuropathology*. 2008; **28**: 561–76.
24. Satoh J, Tabunoki H, Ishida T, Saito Y, Konno H, Arima K. Reactive astrocytes express the potassium channel Kir4.1 in active multiple sclerosis lesions. *Clin Exp Neuroimmunol*. 2013; **4**: 19–28.
25. van der Valk P, De Groot CJ. Staging of multiple sclerosis (MS) lesions: pathology of the time frame of MS. *Neuropathol Appl Neurobiol*. 2000; **26**: 2–10.
26. Satoh J, Tabunoki H, Ishida T, Saito Y, Arima K. Accumulation of a repulsive axonal guidance molecule RGMa in amyloid plaques: a possible hallmark of regenerative failure in Alzheimer's disease brains. *Neuropathol Appl Neurobiol*. 2013; **39**: 109–20.
27. Hanamsagar R, Torres V, Kielian T. Inflammasome activation and IL-1β/IL-18 processing are influenced by distinct pathways in microglia. *J Neurochem*. 2011; **119**: 736–48.
28. Matute C, Torre I, Pérez-Cerdá F, Pérez-Samartín A, Alberdi E, Etxebarria E, et al. $P2X_7$ receptor blockade prevents ATP excitotoxicity in oligodendrocytes and ameliorates experimental autoimmune encephalomyelitis. *J Neurosci*. 2007; **27**: 9525–33.
29. Yiangou Y, Facer P, Durrenberger P, Chessell IP, Naylor A, Bountra C, et al. COX-2, CB2 and P2X7-immunoreactivities are increased in activated microglial cells/macrophages of multiple sclerosis and amyotrophic lateral sclerosis spinal cord. *BMC Neurol*. 2006; **6**: 12.
30. Gandelman M, Peluffo H, Beckman JS, Cassina P, Barbeito L. Extracellular ATP and the $P2X_7$ receptor in astrocyte-mediated motor neuron death: implications for amyotrophic lateral sclerosis. *J Neuroinflammation*. 2010; **7**: 33.
31. Rajamäki K, Nordström T, Nurmi K, Åkerman KE, Kovanen PT, Öörni K, et al. Extracellular acidosis is a novel danger signal alerting innate immunity via the NLRP3 inflammasome. *J Biol Chem*. 2013; **288**: 13410–9.
32. Adachi T, Takahara K, Taneo J, Uchiyama Y, Inaba K. Particle size of latex beads dictates IL-1β production mechanism. *PLoS ONE*. 2013; **8**: e68499.
33. Lööv C, Hillered L, Ebendal T, Erlandsson A. Engulfing astrocytes protect neurons from contact-induced apoptosis following injury. *PLoS ONE*. 2012; **7**: e33090.
34. Fischer MT, Sharma R, Lim JL, Haider L, Frischer JM, Drexhage J, et al. NADPH oxidase expression in active multiple sclerosis lesions in relation to oxidative tissue damage and mitochondrial injury. *Brain*. 2012; **135**: 886–99.
35. Misawa T, Takahama M, Kozaki T, Lee H, Zou J, Saitoh T, et al. Microtubule-driven spatial arrangement of mitochondria promotes activation of the NLRP3 inflammasome. *Nat Immunol*. 2013; **14**: 454–60.
36. Inoue M, Williams KL, Oliver T, Vandenabeele P, Rajan JV, Miao EA, et al. Interferon-β therapy against EAE is effective only when development of the disease depends on the NLRP3 inflammasome. *Sci Signal*. 2012; **5**: ra38.
37. Inoue M, Williams KL, Gunn MD, Shinohara ML. NLRP3 inflammasome induces chemotactic immune cell migration to the CNS in experimental autoimmune encephalomyelitis. *Proc Natl Acad Sci USA*. 2012; **109**: 10480–5.
38. Wang X, Fu S, Wang Y, Yu P, Hu J, Gu W, et al. Interleukin-1β mediates proliferation and differentiation of multipotent neural precursor cells through the activation of SAPK/JNK pathway. *Mol Cell Neurosci*. 2007; **36**: 343–54.

Supporting Information

Additional Supporting Information may be found in the online version of this article:

Figure S1. The specificity of anti-NLRP3, ASC and caspase-1 (CASP1) antibodies.

Figure S2. The expression of NLRP3 inflammasome components in normal control brains.

Table S1. Human brain tissues examined in the present study.

Multiple Sclerosis Journal
http://msj.sagepub.com/

Differential effects of fingolimod on B-cell populations in multiple sclerosis

Masakazu Nakamura, Takako Matsuoka, Norio Chihara, Sachiko Miyake, Wakiro Sato, Manabu Araki, Tomoko Okamoto, Youwei Lin, Masafumi Ogawa, Miho Murata, Toshimasa Aranami and Takashi Yamamura

Mult Scler published online 13 February 2014
DOI: 10.1177/1352458514523496

The online version of this article can be found at:
http://msj.sagepub.com/content/early/2014/02/18/1352458514523496.citation

Published by:
SAGE
http://www.sagepublications.com

Research Paper

MULTIPLE SCLEROSIS JOURNAL | MSJ

Multiple Sclerosis Journal
1–10

DOI: 10.1177/1352458514523496
msj.sagepub.com
SAGE

Differential effects of fingolimod on B-cell populations in multiple sclerosis

Masakazu Nakamura[1,2], Takako Matsuoka[1], Norio Chihara[1], Sachiko Miyake[1,3], Wakiro Sato[3,4], Manabu Araki[3], Tomoko Okamoto[3,4], Youwei Lin[1,3,4], Masafumi Ogawa[3,4], Miho Murata[4], Toshimasa Aranami[1,3] and Takashi Yamamura[1,3]

Abstract

Background: Fingolimod is an oral drug approved for multiple sclerosis (MS) with an ability to trap central memory T cells in secondary lymphoid tissues; however, its variable effectiveness in individual patients indicates the need to evaluate its effects on other lymphoid cells.

Objective: To clarify the effects of fingolimod on B-cell populations in patients with MS.

Methods: We analysed blood samples from 9 fingolimod-treated and 19 control patients with MS by flow cytometry, to determine the frequencies and activation states of naive B cells, memory B cells, and plasmablasts.

Results: The frequencies of each B-cell population in peripheral blood mononuclear cells (PBMC) were greatly reduced 2 weeks after starting fingolimod treatment. Detailed analysis revealed a significant reduction in activated memory B cells ($CD38^{int\text{-}high}$), particularly those expressing Ki-67, a marker of cell proliferation. Also, we noted an increased proportion of activated plasmablasts ($CD138^{+}$) among whole plasmablasts, in the patients treated with fingolimod.

Conclusions: The marked reduction of Ki-67^{+} memory B cells may be directly linked with the effectiveness of fingolimod in treating MS. In contrast, the relative resistance of $CD138^{+}$ plasmablasts to fingolimod may be of relevance for understanding the differential effectiveness of fingolimod in individual patients.

Keywords

B cells, CD38, CD138, fingolimod, memory B cell, multiple sclerosis, plasmablast, proliferation, resistance, sphingosine 1-phosphate receptor 1

Date received: 5 September 2013; accepted: 16 January 2014

Introduction

It is currently assumed that a large proportion of autoreactive T cells in multiple sclerosis (MS) is derived from a pool of $CCR7^{+}$ central memory T cells that are passing through the secondary lymphoid tissues (SLT).[1] Accordingly, egress of the T cells from the SLT represents a key process in MS pathogenesis. This process follows a rule of chemotaxis, in which the sphingosine 1-phosphate (S1P) receptor 1 (S1P1) expressed by lymphocytes is critically involved.[2] Fingolimod, an oral drug for treating relapsing–remitting MS (RRMS), serves as a functional antagonist for S1P1: Fingolimod induces internalisation and degradation of S1P1 in lymphocytes, causing the lymphocytes to lose the ability to respond to S1P and consequently, to become trapped in the SLT.[3] Analysis of large cohorts of patients with RRMS demonstrate the overall effectiveness of fingolimod in reducing the annualised relapse rate (ARR), as well as the appearance of new brain lesions in the patients' magnetic resonance imaging (MRI) scans.[4,5]

The number of central memory interleukin 17-producing $CD4^{+}$ T cells (Th17 cells) is reduced in the peripheral blood of fingolimod-treated patients. This is now being interpreted as a major mechanism of drug action;[6] however, fingolimod is not able to prevent relapses nor exhibit

[1]Department of Immunology, National Institute of Neuroscience, National Centre of Neurology and Psychiatry (NCNP), Tokyo, Japan.
[2]Department of Neurology, Graduate School of Medicine, Kyoto University, Kyoto, Japan.
[3]Multiple Sclerosis Centre, National Centre Hospital, NCNP, Tokyo, Japan.
[4]Department of Neurology, National Centre Hospital, NCNP, Tokyo, Japan.

Corresponding author:
Takashi Yamamura, Department of Immunology, National Institute of Neuroscience, National Centre of Neurology and Psychiatry, 4-1-1 Ogawahigashi, Kodaira, Tokyo 187-8502, Japan.
Email: yamamura@ncnp.go.jp

Table 1. Clinical data of the patients in this study.

Patient	Gender	Age (years)	Duration (years)	Relapse frequency (last 2 yrs)	EDSS	DMT before initiation of fingolimod	Complications
1	M	34	7	5	1.5	IFNβ1a + PSL	Asthma
2	M	43	6	2	2.5	PSL	Graves' disease
3	M	39	5	1	3.5	None	Depression
4	M	41	13	1	3.5	IFNβ1b	None
5	M	29	2	3	2.0	IFNβ1b	Pectus excavatum
6	F	41	24	6	3.5	IFNβ1b → GA → Dex	Depression
7	M	56	16	2	5.5	IFNβ1b → IFNβ1b + PSL → IFNβ1a + AZP	Osteoporosis
8	M	41	9	2	4.0	IFNβ1b → IFNβ1a	Depression
9	M	60	20	1	3.5	AZP → MZR → IFNβ1b	None
mean ± SD		42.7 ± 9.8	11.3 ± 7.4	2.5 ± 1.8	3.3 ± 1.2		

AZP: Azathioprine; Dex: dexamethasone; DMT: disease-modifying treatment; EDSS: Expanded Disability Status Scale; F: female; GA: glatiramer acetate; IFN: interferon; M: male; MZR: mizoribine; PSL: prednisolone.

appreciable effectiveness in all patients. In fact, recent case reports document the presence of fingolimod-treated MS patients who have developed tumefactive brain lesions, after receiving fingolimod.[7–10] Moreover, clinical worsening accompanied by large brain lesions is described in patients with neuromyelitis optica (NMO), within months of starting fingolimod.[11,12] Our current understanding of fingolimod-related biology therefore remains incomplete, particularly regarding differential effectiveness in individual patients.

Not only the presence of clonally-expanded B cells in the central nervous system (CNS),[13,14] but the efficacy of the anti-CD20 monoclonal antibody (mAb) rituximab[15] rationally indicates the involvement of B cells in the pathogenesis of MS. Therefore, B-cell migration can serve as a therapeutic target in MS, so we were prompted to investigate whether inhibition of B-cell migration may explain the differential effectiveness of fingolimod. Because the effects of fingolimod on B cells in MS have not been fully characterised,[16] we analysed the alterations of B-cell populations in fingolimod-treated RRMS patients by flow cytometry, measuring the frequencies and activation states of their peripheral blood B-cell populations.

Materials and methods

Patients and sample collection

The following subjects were enrolled in the Multiple Sclerosis Clinic of the National Centre of Neurology and Psychiatry (NCNP) in Japan:

(a) Fingolimod-naïve patients with RRMS ($n = 9$);
(b) RRMS patients who were treated with other disease-modifying treatments (DMTs) or corticosteroids ($n = 19$); and
(c) Healthy donors ($n = 3$).

All MS patients fulfilled the revised McDonald criteria.[17] Fingolimod (0.5 mg once/day) was administered to nine fingolimod-naïve patients. These patient's blood samples were collected before and 2 weeks after initiating fingolimod therapy. Most of these patients discontinued other DMTs at least 2 weeks before entry into the study, due to non-responsiveness to their DMT treatment or due to adverse events. The absence of serum anti-aquaporin 4 (AQP4)-Ab was confirmed by cell-based assays.[18,19] Upon MRI, no patient showed longitudinally-extensive spinal cord lesions extending over three or more vertebrae. The clinical data of these nine patients are summarised in Table 1.

Control blood samples were collected from 19 patients with RRMS (mean age ± SD: 41.8 ± 13.8 years; female:male ratio: 15:4) who had not been exposed to fingolimod before nor during the study. The three healthy donors were males (mean age ± SD: 40.0 ± 3.6 years). This study was approved by the Ethics Committee of the NCNP. We obtained written informed consent from all subjects.

Reagents

The following fluorescence- or biotin-labelled mAbs were used: anti-CD19-allophycocyanin (APC)-cyanine 7 (Cy7), anti-CD27-V500 and anti-CD27-phycoerythrin (PE)-Cy7 (BD Biosciences, San Jose, CA, USA); anti-CD180-PE and anti-CCR7-fluorescein isothiocyanate (FITC) (BD Pharmingen, San Jose, CA, USA); anti-CD38-FITC, anti-CD3-FITC and mouse IgG1-FITC (Beckman Coulter, Brea, CA, USA); anti-CD138-APC, mouse IgG1κ-APC, anti-HLA-DR-Pacific Blue, mouse IgG2Aκ-Pacific Blue, anti-CD183 (CXCR3)-peridinin-chlorophyll-protein (PerCp)-cyanine 5.5 (Cy5.5), mouse IgG1κ-PerCp-Cy5.5, anti-CD38-APC, anti-CD38-PerCp-Cy5.5, anti-CD14-Pacific Blue, anti-Ki-67-Brilliant Violet, mouse IgG1κ-Brilliant Violet and streptavidin-PE-Cy7 (BioLegend, San

Diego, CA, USA); and anti-CXCR4-biotin and mouse IgG2A-biotin (R&D Systems, Minneapolis, MN, USA).

Cell preparation and flow cytometry

Peripheral blood mononuclear cells (PBMC) were isolated by density gradient centrifugation, using Ficoll–Paque Plus (GE Healthcare Bioscience, Oakville, ON, Canada). B-cell populations were defined in reference to our previous paper,[19] as follows: total B cells, $CD19^+$; naïve B cells (nBs), $CD19^+CD27^-$; memory B cells (mBs), $CD19^+CD27^+CD180^+$; and plasmablasts (PBs), $CD19^+CD27^+CD180^-CD38^{high}$.

To evaluate the frequency and activation state of each B-cell population, PBMC were stained with anti-CD19-APC-Cy7, anti-CD27-V500, anti-CD38-FITC, anti-CD180-PE, anti-CD138-APC, anti-CXCR3-PerCp-Cy5.5, anti-CXCR4-biotin, streptavidin-PE-Cy7 and anti-HLA-DR-Pacific Blue. To assess the expression of CCR7 in each B cell population, PBMC were stained with anti-CD19-APC-Cy7, anti-CD27-PE-Cy7, anti-CD38-APC, anti-CD180-PE and anti-CCR7-FITC.

For examining Ki-67 expression in each B-cell population, PBMC were stained with anti-CD19-APC-Cy7, anti-CD27-PE-Cy7, anti-CD38-PerCp-Cy5.5, anti-CD180-PE and anti-CD138-APC, then fixed in phosphate-buffered saline (PBS) containing 2% paraformaldehyde and permeabilised with 0.1% saponin. Subsequently, these cells were stained with anti-Ki-67-Brilliant Violet. We used the appropriate isotype control antibodies as negative controls for each staining. At the end of the incubation, the cells were washed and resuspended in PBS supplemented with 0.5% bovine serum albumin (BSA) and analysed by FACS Canto II (BD Biosciences), according to the manufacturer's instructions.

Cell sorting

PBMC were labelled with CD3 and CD14 microbeads (Miltenyi Biotec, Bergisch Gladbach, Germany) and then separated into positive and negative fractions by AutoMACS (Miltenyi Biotec). The positive fraction was stained with anti-CD3-FITC and anti-CD14-Pacific Blue, whereas the negative fraction was stained with anti-CD19-APC-Cy7, anti-CD27-PE-Cy7, anti-CD38-APC and anti-CD180-PE. Each positive and negative fraction was sorted into $CD3^+$ T cells and $CD14^+$ monocytes, or into nBs, mBs and PBs by a FACS Aria II cell sorter (BD Biosciences). The purity of the sorted cells was > 95%.

Quantitative real-time PCR

Messenger ribonucleic acid (mRNA) was prepared from the sorted cells using the RNeasy Kit (Qiagen, Tokyo, Japan), further treated with DNase using the RNase-Free DNase Set (Qiagen), and reverse-transcribed to complementary DNA (cDNA) using the cDNA Synthesis Kit (Takara Bio, Shiga, Japan). We performed polymerase chain reaction (PCR) using iQ SYBR Green Supermix (Takara Bio) on a LightCycler (Roche Diagnostics, Indianapolis, IN, USA). RNA levels were normalised to endogenous β-actin (ACTB) for each sample. The following primers were used: S1P1 forward, CGAGAGCACTACGCAGTCAG; and S1P1 reverse, AGAGCCTTCACTGGCTTCAG.

Data analysis and statistics

We used Diva software (BD Biosciences) to analyse our flow cytometry data. We performed the statistical analysis with Prism software (GraphPad Software, San Diego, CA, USA). Paired or unpaired *t*-tests were used once the normality of the data was confirmed by the Kolmogorov-Smirnov test. Otherwise, the Wilcoxon signed-rank test or the Mann-Whitney *U*-test was used, as appropriate. One-way analysis of variance (ANOVA) was used to compare data from more than two groups. If the one-way ANOVA was significant, we performed *post hoc* pairwise comparisons using Tukey's test. A p value < 0.05 was considered statistically significant.

Results

B-cell populations express S1P1 mRNA

First, we used flow cytometry to examine S1P1 expression on the surfaces of the B-cell populations; however, surface S1P1 was hardly detected (data not shown). This is probably because of its internalisation following S1P binding. In support of this, it is known that S1P is abundantly present in peripheral blood.[2] Thus, we measured S1P1 mRNA in purified lymphocyte populations from the PBMCs of three healthy donors. Each B-cell population was identified by flow cytometry, as shown in Figure 1(a). We found that comparable levels of S1P1 mRNA were expressed in T cells, nBs and mBs. In comparison, PBs expressed a significantly lower level of S1P1, and S1P1 expression in monocytes was virtually absent (Figure 1(b)). Of note, a lower S1P1 expression by PBs, as compared with other B cell populations, is also described in mice.[20,21] These S1P1 mRNA expression profiles suggested that not only T cells, but B-cell migration, could also be influenced by fingolimod.

Next, we measured the frequencies of the B-cell populations in the PBMCs from nine patients with RRMS, before and 2 weeks after starting fingolimod. Results of flow cytometry showed that the frequencies of nBs, mBs and PBs among PBMCs were significantly decreased after initiating fingolimod treatment (Figure 1(c)). We confirmed that the absolute numbers of each population in the peripheral blood were also significantly decreased after starting fingolimod (Figure 1(d)). The mean decrease rate ± SD of each cell population was calculated based on the absolute cell number, giving the following results: total B cells, 87.6 ± 5.8%; nBs, 88.1 ± 6.0%; mBs, 85.4 ± 9.1% and PBs, 89.8

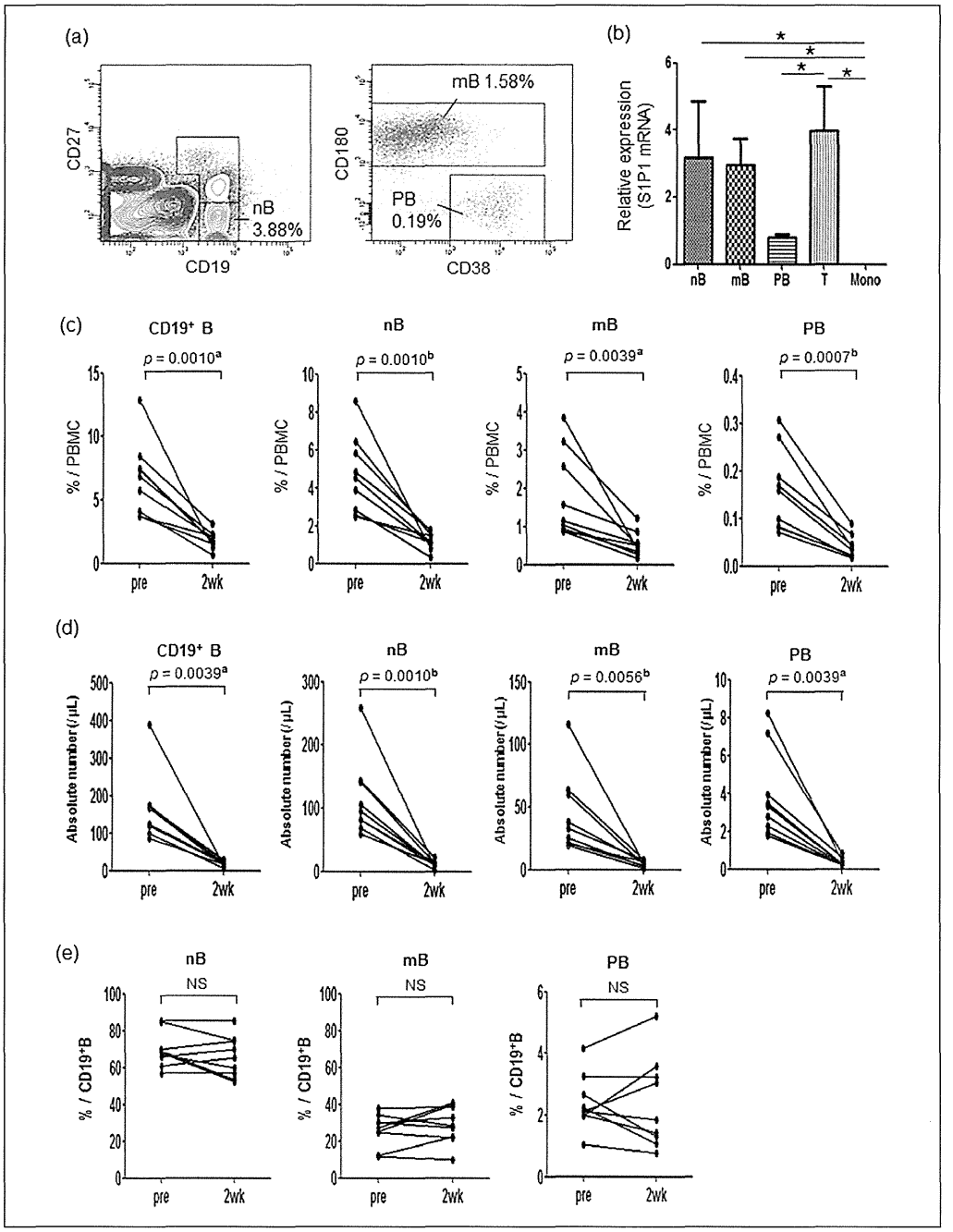

Figure 1. Frequency and absolute number of each B-cell population found in peripheral blood from MS patients.
(a)Representative flow cytometry scheme to analyse B-cell populations in PBMC. The PBMC were simultaneously stained with fluorescence-conjugated anti-CD19, -CD27, -CD38 and -CD180 mAbs. The gate for $CD19^+CD27^-$ nBs is shown in the left panel. The $CD19^+CD27^+$ fraction partitioned in the left panel was analysed for CD180 and CD38 expression to specify $CD180^+$ cells (mBs), and for $CD180^-CD38^{high}$ cells (PBs) in the right panel. Values represent frequencies of B-cell populations in PBMC. Total $CD19^+$ B cell counts were calculated by summing the frequencies of the partitioned populations in the left panel. (b) Each B-cell population, $CD3^+$ T cells and $CD14^+$ monocytes in PBMCs from three healthy donors were sorted by FACS, and S1P1 mRNA expression levels were determined by quantitative RT-PCR. Data were normalised to the amount of ACTB for each sample. Data are represented as mean relative expression ± SD. *$p < 0.05$ by one-way ANOVA and *post hoc* Tukey's test. (c), (d), and (e) Data shown are the frequencies of B-cell populations in PBMC (c), the absolute numbers of B cell populations in peripheral blood (d) and the frequencies of B-cell populations in $CD19^+$ B cells (e) from nine patients with MS before (pre) and 2 weeks after (2 wk) initiating fingolimod. Data from the same patients are connected with lines.
$p^a < 0.05$ by Wilcoxon signed-rank test.
$p^b < 0.05$ by paired *t*-test.
ACTB: endogenous beta actin; ANOVA: analysis of variance; FACS: Fluorescence-activated cell sorting; mAbs: monoclonal antibodies; mBs: memory B cells; mono: monocytes; mRNA: messenger ribonucleic acid; MS: multiple sclerosis; nBs: naïve B cells; NS: not statistically significant; PBMC: peripheral blood mononuclear cells; PBs: plasmablasts; pre: before treatment; RT-PCR: reverse transcriptase - polymer chain reaction; S1P1: sphingosine 1 phosphate receptor 1; T: T cells; 2 wk: 2 weeks after treatment initiation

± 3.3%. Thus, all B-cell populations decreased at similar rates, regardless of their S1P1 expression levels. We also noticed that reduction of the B-cell populations did not correlate with CCR7 expression (a large proportion of nBs and mBs expresses CCR7, whereas only a small percentage of PBs expresses CCR7 (Supplementary Figure 1)). Consistently, the frequency of each B-cell population within $CD19^+$ B cells was not significantly altered in the fingolimod-treated patients (Figure 1(e)).

$CD38^{int}$- and $CD38^{high}$-activated memory B cells are preferentially decreased in fingolimod-treated patients

We next assessed mBs, which are assumed to play an important role in MS.[22,23] To evaluate the effects of fingolimod on the activation state of mBs, we first analysed CD38 expression of mBs in the nine patients, before and after initiating fingolimod. CD38 is a marker that is upregulated upon B-cell activation.[24] We found that mBs could be classified into three subpopulations according to CD38 expression levels ($CD38^{low}$, $CD38^{int}$ and $CD38^{high}$). Notably, frequencies of $CD38^{int}$ and $CD38^{high}$ mBs were significantly decreased 2 weeks after initiating fingolimod, whereas the frequency of the $CD38^{low}$ subpopulation became significantly increased (Figure 2(a) and (b)).

We further examined the expression of another activation marker, HLA-DR, within the $CD38^{low}$, $CD38^{int}$ and $CD38^{high}$ mB subpopulations. We found that the $CD38^{high}$ subpopulation expressed a significantly higher level of HLA-DR, compared with the $CD38^{low}$ mB population, as assessed by mean fluorescence intensities (MFIs) (Figure 2(c) and (d)). Although not statistically significant, HLA-DR expression in the $CD38^{int}$ subpopulation was intermediate, compared with that in the $CD38^{low}$ mB subpopulation. We also found that the MFIs of forward scatter (FSC), which reflects cell size, were significantly higher in the $CD38^{high}$ subpopulation, compared with the $CD38^{low}$ and $CD38^{int}$ subpopulations (Figure 2(c) and (d)). These findings suggest that $CD38^{high}$ mBs may contain a larger number of recently-activated blastic cells.

Fingolimod reduced Ki-67^+ recently-activated memory B cells in peripheral blood

The nuclear antigen Ki-67 is exclusively expressed in the active stages of the cell cycle (G1, S, G2 and M phases),[25] and Ki-67^+ circulating immune cells are considered to be recently activated cells that have just egressed from the SLT. To clarify whether $CD38^{high}$ and $CD38^{int}$ mB subpopulations are enriched for recently-activated cells, we examined the frequency of Ki-67^+ cells in each mB subpopulation, in the six MS patients who were not treated with fingolimod. This analysis revealed that $CD38^{high}$ mBs contained a significantly higher frequency of Ki-67^+ cells than did $CD38^{low}$ and $CD38^{int}$ mBs, and that $CD38^{int}$ mBs were likely to contain a higher frequency of Ki-67^+ cells than the $CD38^{low}$ mBs (Figure 3(a) and (b)). In addition, we compared the frequency of Ki-67^+ cells in each mB subpopulation, between fingolimod-treated (n = 5) and -untreated control patients (n = 6), and found that $CD38^{int}$ and $CD38^{high}$ mBs of the fingolimod-treated patients contained a significantly lower percentage of Ki-67^+ cells compared with those of the untreated patients (Figure 3(c)). These findings suggest that recently activated mBs are enriched in $CD38^{int}$ and $CD38^{high}$ subpopulations and that fingolimod efficiently blocks the egress of these cells from the SLT into the peripheral circulation.

The $CD138^+$ subpopulation in plasmablasts is relatively resistant to fingolimod

Finally, we analysed alterations of PBs by fingolimod in more detail. As PBs serve as migratory B cells that produce pathogenic autoantibody directed against AQP4,[19] their role in the antibody-mediated pathology is being considered also in the pathogenesis of MS. Notably, CD138 expression appears to separate PB subpopulations that could become differentially altered during the inflammatory process. In fact, $CD138^+$ PBs have a higher potential to migrate to inflamed tissues than $CD138^-$ PBs.[26] Moreover, as has recently been reported by us, $CD138^+$HLA-DR^+ PBs are selectively enriched in the cerebrospinal fluid (CSF) during relapse of NMO, and the $CD138^+$HLA-DR^+ PBs migrating to the CSF express CXCR3.[27] Therefore, we compared the frequencies of $CD138^+$ cells in PBs, as well as their expression of HLA-DR and CXCR3, before and after fingolimod treatment.

We found that the frequencies of $CD138^+$ PBs among total PBs were significantly increased after fingolimod initiation (Figure 4(a) and (b)); however, the absolute numbers of both subpopulations decreased, implying that $CD138^+$ PBs are relatively resistant to fingolimod, compared with $CD138^-$ PBs (Supplementary Figure 2(a) and (b)). After initiating fingolimod, $CD138^-$ PBs showed lower expression of HLA-DR, whereas the percentages of $CXCR3^+$ cells remained unchanged (Figure 4(c) – (e)). In contrast, fingolimod treatment did not significantly reduce the expression level of HLA-DR among $CD138^+$ PBs. More interestingly, $CD138^+$ PBs became more enriched with $CXCR3^+$ cells after initiating fingolimod (Figure 4(c) – (e)). The definition of PBs as $CD19^+CD27^+CD180^-CD38^{high}$ cells in this study was modified to efficiently specify autoantibody-producing cells;[19] however, adopting a more commonly used definition of PBs as $CD19^+CD27^+CD38^{high}$ cells did not alter the results (Supplementary Figure 3(a) – (e)).

Discussion

Previous studies show that fingolimod markedly decreases the number of T and B cells in the peripheral blood, without

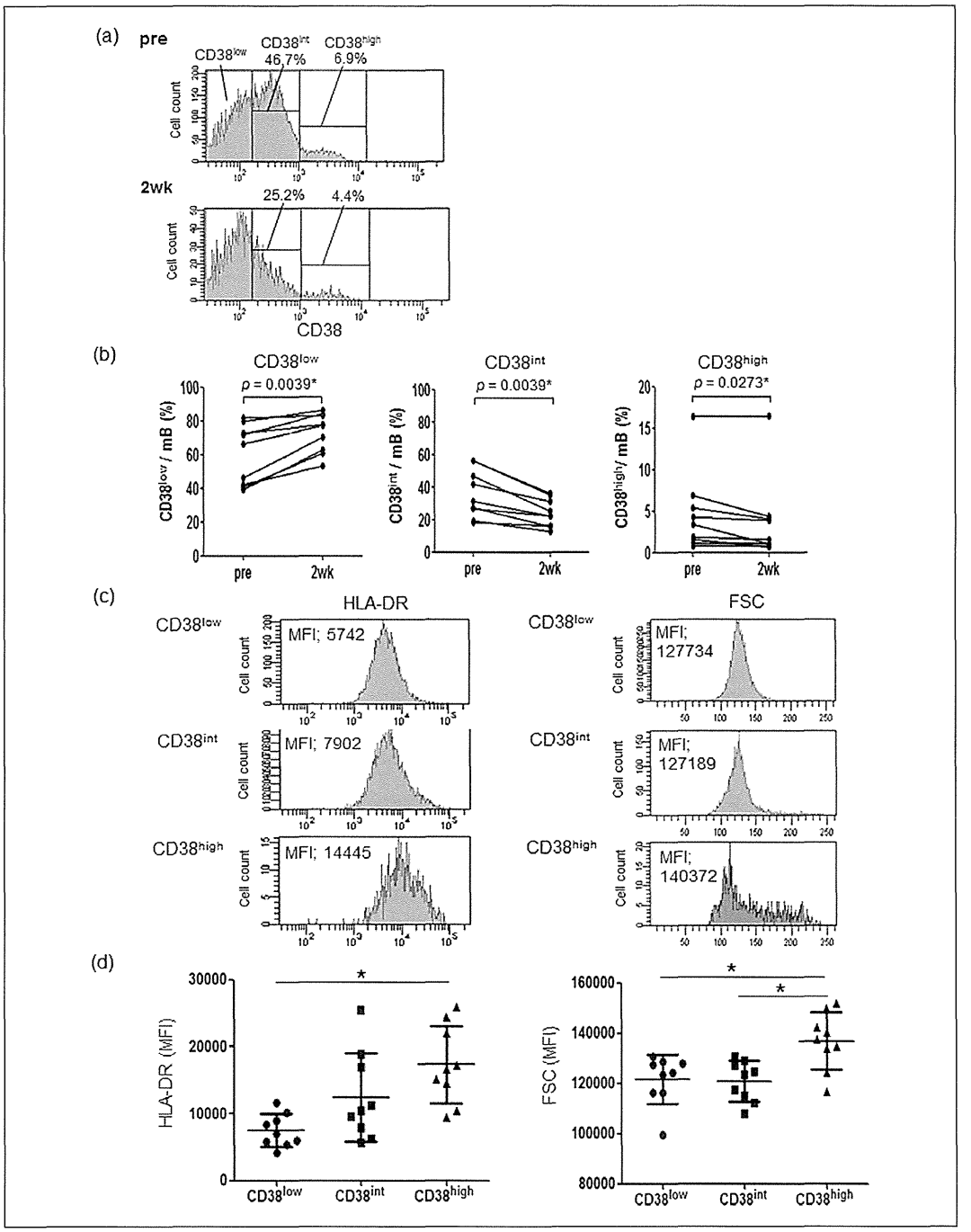

Figure 2. Frequency and activation state of each mB subpopulation in the peripheral blood of MS patients.
(a)Representative histograms of CD38 expression in mB of peripheral blood from a fingolimod-treated patient. Upper (pre) and lower (2wk) panels show the histograms before and 2 weeks after fingolimod initiation, respectively. The two values above each histogram indicate frequencies of the mB subpopulations with intermediate ($CD38^{int}$, left) and high ($CD38^{high}$, right) CD38 expression. (b) Data shown are frequencies of mB subpopulations, classified by CD38 expression levels ($CD38^{low}$ (left panel), $CD38^{int}$ (middle panel) and $CD38^{high}$ (right panel)), in the peripheral blood from nine patients with MS, before (pre) and 2 weeks after (2wk) fingolimod initiation. Data from the same patients are connected with lines. *$p < 0.05$ by Wilcoxon signed-rank test. (c) Representative histograms of HLA-DR (left column) and FSC (right column) expression in each mB subpopulation ($CD38^{low}$ (upper row), $CD38^{int}$ (middle row) and $CD38^{high}$ (lower row)) of peripheral blood from a patient with MS, before fingolimod initiation. Values represent MFIs of HLA-DR and FSC. (d) Data shown are MFI of HLA-DR (left panel) and FSC (right panel) in mB subpopulations ($CD38^{low}$, $CD38^{int}$ and $CD38^{high}$) of peripheral blood from nine patients with MS, before fingolimod treatment. Data are represented as mean ± SD.
*$p < 0.05$ by one-way ANOVA and *post hoc* Tukey's test.
ANOVA: analysis of variance; FSC: forward scatter; HLA: human leukocyte antigen; mB: memory B cells; MFI: mean fluorescence intensity; MS: multiple sclerosis; pre: before treatment; 2wk: 2 weeks after treatment initiation

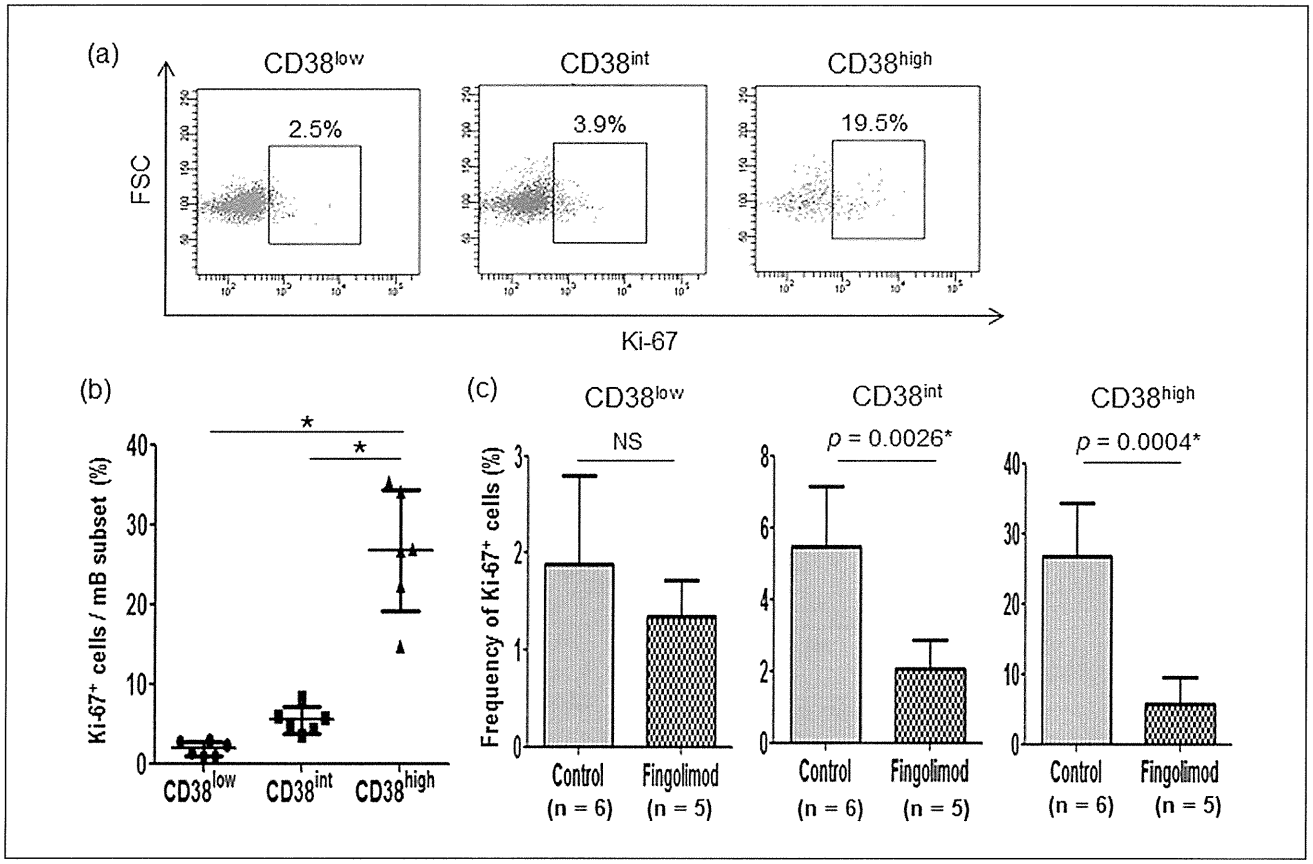

Figure 3. Ki-67 expression in mB subpopulations of peripheral blood from MS patients.
(a)Representative flow cytometry analyses of intracellular Ki-67 expression in mB subpopulations ($CD38^{low}$ (left panel), $CD38^{int}$ (middle panel), and $CD38^{high}$ (right panel)) of peripheral blood from an untreated patient with MS. Each mB subpopulation was analysed for FSC and Ki-67 expression. Values in each plot represent frequency of $Ki\text{-}67^+$ cells in each mB subpopulation. (b) Frequency of $Ki\text{-}67^+$ cells in each mB subpopulation of peripheral blood from six untreated patients with MS. Data are represented as mean ± SD. $^*p < 0.05$ by one-way ANOVA and *post hoc* Tukey's test. (c) Frequency of the $Ki\text{-}67^+$ population in each mB subpopulation ($CD38^{low}$ (left panel), $CD38^{int}$ (middle panel), and $CD38^{high}$ (right panel)) is compared between untreated patients with MS (control; $n = 6$) and fingolimod-treated patients with MS (Fingolimod; $n = 5$). Mean duration with fingolimod treatment ± SD is 15.8 ± 8.8 (6 to 30) weeks. Data are represented as mean ± SD.
$^*p < 0.05$ by unpaired *t*-test.
FSC: forward scatter; Ki-67: a marker present only during cell growth or proliferation; mB: memory B cells; MS: multiple sclerosis; NS: not statistically significant.

affecting the total numbers of monocytes and natural killer (NK) cells.[16,28,29] Furthermore, in MS, fingolimod selectively reduces naïve T cells, as well as $CD4^+$ central memory T cells that are enriched for Th17 cells.[6,30] In addition, fingolimod treatment may induce a relative increase in $CD27^-CD28^-$ $CD8^+$ T cells[31] and a decrease in $CD56^{bright}CD62L^+CCR7^+$ NK cells.[32]

The role of autoreactive $CD4^+$ T cells in MS pathogenesis has been emphasised over decades.[33] In contrast, B-cell involvement in MS was highlighted lately, after the clinical effectiveness of rituximab was demonstrated in RRMS patients. Rituximab's effectiveness in MS may result from the depletion of autoantibody-producing B cells, but it can also be explained by depletion of B cells that are able to induce or support activation of autoreactive T cells.[15] In fact, B cells exhibit the ability to present antigen to T cells, and mBs are more capable than nBs of supporting the proliferation of neuroantigen-specific $CD4^+$ T cells, in vitro.[23] The presence of oligoclonal bands in the CSF suggests local production of antibodies within the CNS.[34] Consistent with this, brain lesions[13] and CSF[14] of patients with MS contain clonally-expanded B cells. These results collectively support the postulate that mBs can potentially trigger the inflammation of MS, either via autoantibody production or via autoantigen presentation to autoreactive T cells.

The focus of this study is to investigate the alterations of peripheral blood B-cell types in fingolimod-treated patients with RRMS. We showed that activated $CD38^{int}$ and $CD38^{high}$ mB subpopulations were highly susceptible to

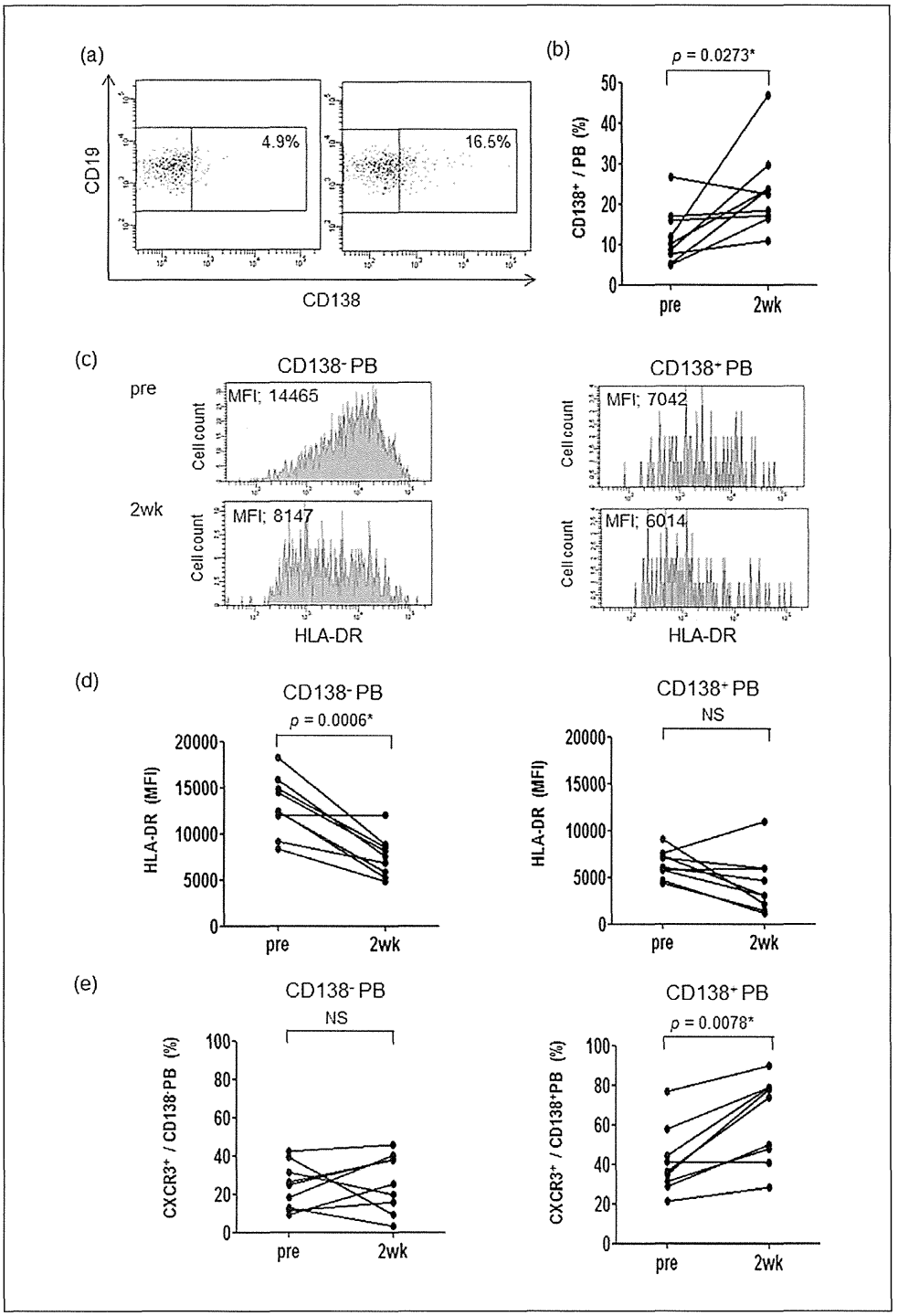

Figure 4. Phenotypic alteration of the remaining PBs in peripheral blood following fingolimod treatment.
(a)Representative dot plots of $CD19^+CD27^+CD180^-CD38^{high}$ PB, analysed for CD19 and CD138 expression before (pre) and 2 weeks after (2wk) fingolimod initiation. Values represent frequencies of the $CD138^+$ subpopulation in total PB. (b) Data are frequencies of the $CD138^+$ subpopulation in total PB of peripheral blood from nine patients with MS before (pre) and 2 weeks after (2wk) fingolimod initiation. Data from the same patients are connected with lines. *$p < 0.05$ by Wilcoxon signed-rank test. (c) Data are representative histograms of HLA-DR expression in $CD138^-$ and $CD138^+$ PB of peripheral blood, from a patient with MS before (pre) and 2 weeks after (2wk) fingolimod initiation. Values represent MFI of HLA-DR. (d) Data are MFI of HLA-DR in $CD138^-$ and $CD138^+$ PB of peripheral blood from nine patients with MS, before (pre) and 2 weeks after (2wk) fingolimod initiation. Data from the same patients are connected with lines. *$p < 0.05$ by paired t-test. (e) Data are frequencies of $CXCR3^+$ cells in $CD138^-$ PB and $CD138^+$ PB of peripheral blood from nine patients with MS before (pre) and 2 weeks after (2wk) fingolimod initiation. Data from the same patients are connected with lines. *$p < 0.05$ by Wilcoxon signed-rank test.
MFI: mean fluorescence intensity; MS: multiple sclerosis; NS: not statistically significant; PB: plasmablast; pre: before treatment; 2wk: after 2 weeks of treatment

fingolimod, as indicated by their reduction in the peripheral blood following fingolimod treatment. It is demonstrated in mice that surface expression levels of S1P1 on B cells in the SLT are controlled by transcription levels and CD69-mediated internalisation of S1P1. Stimulation of B-cell receptors induces not only a cessation of S1P1 transcription, but also an upregulation of CD69. Both of these changes reduce the expression levels of surface S1P1 in the SLT to some extent.[2]

Although we were not able to directly analyse B cells in the SLT of the patients, we speculated that surface S1P1 expression on mBs within the SLT in human may also decrease greatly, following antigen activation and exposure to fingolimod, which would result in these B lymphocytes having a reduced responsiveness to S1P. In fact, the activated mB subpopulations that we isolated from the patients' peripheral blood, in particular $CD38^{high}$ mB, were found to contain a substantial proportion of $Ki\text{-}67^+$ cells (Figure 3(a) and (b)). We confirmed that the proportions of $Ki\text{-}67^+$ cells in the activated $CD38^{int}$ and $CD38^{high}$ mB subpopulations were significantly decreased following fingolimod treatment, suggesting that recently-activated cells were selectively trapped in the SLT following fingolimod treatment. Because activation of autoreactive mBs in the SLT followed by their migration to the CNS could trigger a relapse of RRMS,[35] we assumed that inhibition of activated mB cell egress from the SLT was at least partly involved in the reduced relapses of RRMS after fingolimod treatment.

We also identified a PB subpopulation that is relatively resistant to fingolimod as being $CD138^+$ PBs. The frequency of the $CD138^+$ subpopulation in the total PBs, and that of $CXCR3^+$ cells in $CD138^+$ PBs, was significantly increased by fingolimod treatment. Of note, the $CD138^+CXCR3^+$ PBs are enriched in the CSF of NMO during relapse,[27] and fingolimod could induce exacerbation of NMO, accompanied by the appearance of large brain lesions.[11,12] Although knowledge on the biology of PBs is limited, the percentages of $CCR7^+$ cells are much lower as compared with nBs or mBs, indicating that fingolimod may differentially alter the in vivo migration of PBs and other B cells.

It is of relevance to note that despite reductions of circulating lymphocytes, RRMS patients receiving fingolimod may develop clinical relapses. These relapses are not always mild, but could be serious and accompany huge brain lesions.[7–10] Although the trapping of regulatory lymphocytes in the SLT[8,9] or the enrichment for $CD45RO^-CCR7^-CD8^+$ T cells in the CSF[7] is proposed as a possible mechanism for formation of tumefactive brain lesions, we were very curious to know if the increased proportion of $CD138^+$ PBs over other lymphocytes in the peripheral blood might influence the character of the CNS pathology and induce large demyelinating lesions. In fact, it was recently reported that $CD45^+CD19^+CD138^+$ PBs are relatively enriched in the CSF of fingolimod-treated MS patients,[16] raising the possibility that the dominance of $CD138^+$ PBs in the peripheral blood is preserved or even promoted in the CNS of patients with MS who develop tumefactive brain lesions[7–10] and NMO patients who deteriorate[11,12] after being treated with fingolimod. Therefore, resistance of activated PBs in fingolimod-treated patients with MS or NMO may give us a clue to understanding the individual patients' differences regarding the effectiveness of fingolimod therapy.

Acknowledgements

We thank Toshiyuki Takahashi at the Department of Neurology, Tohoku University, for examining serum anti-AQP4-Abs in our patients. We also thank Hiromi Yamaguchi, Yasuko Hirakawa, and Tomoko Ozawa for their technical support.

Conflict of interest

The authors declare that there are no conflicts of interest.

Funding

This work was supported by the Ministry of Health, Labour and Welfare of Japan (grant on intractable neuroimmunological diseases number H23-nanchi-ippan-017); and the Japanese Society for the Promotion of Science (grant number: S24229006).

References

1. Kivisakk P, Mahad DJ, Callahan MK, et al. Expression of CCR7 in multiple sclerosis: Implications for CNS immunity. *Ann Neurol* 2004; 55: 627–638.
2. Cyster JG and Schwab SR. Sphingosine-1-phosphate and lymphocyte egress from lymphoid organs. *Ann Rev Immunol* 2012; 30: 69–94.
3. Cohen JA and Chun J. Mechanisms of fingolimod's efficacy and adverse effects in multiple sclerosis. *Ann Neurol* 2011; 69: 759–777.
4. Kappos L, Radue EW, O'Connor P, et al. A placebo-controlled trial of oral fingolimod in relapsing multiple sclerosis. *N Engl J Med* 2010; 362: 387–401.
5. Cohen JA, Barkhof F, Comi G, et al. Oral fingolimod or intramuscular interferon for relapsing multiple sclerosis. *N Engl J Med* 2010; 362: 402–415.
6. Mehling M, Lindberg R, Raulf F, et al. Th17 central memory T cells are reduced by FTY720 in patients with multiple sclerosis. *Neurology* 2010; 75: 403–410.
7. Pilz G, Harrer A, Wipfler P, et al. Tumefactive MS lesions under fingolimod: A case report and literature review. *Neurology* 2013; 81: 1654–1658.
8. Jander S, Turowski B, Kieseier BC, et al. Emerging tumefactive multiple sclerosis after switching therapy from natalizumab to fingolimod. *Mult Scler* 2012; 18: 1650–1652.
9. Visser F, Wattjes MP, Pouwels PJ, et al. Tumefactive multiple sclerosis lesions under fingolimod treatment. *Neurology* 2012; 79: 2000–2003.
10. Leypoldt F, Munchau A, Moeller F, et al. Hemorrhaging focal encephalitis under fingolimod (FTY720) treatment: A case report. *Neurology* 2009; 72: 1022–1024.

11. Izaki S, Narukawa S, Kubota A, et al. [A case of neuromyelitis optica spectrum disorder developing a fulminant course with multiple white-matter lesions, following fingolimod treatment]. *Rinsho Shinkeigaku* 2013; 53: 513–517.
12. Min JH, Kim BJ and Lee KH. Development of extensive brain lesions following fingolimod (FTY720) treatment in a patient with neuromyelitis optica spectrum disorder. *Mult Scler* 2012; 18: 113–115.
13. Baranzini SE, Jeong MC, Butunoi C, et al. B-cell repertoire diversity and clonal expansion in multiple sclerosis brain lesions. *J Immunol* 1999; 163: 5133–5144.
14. Qin Y, Duquette P, Zhang Y, et al. Clonal expansion and somatic hypermutation of V(H) genes of B cells from cerebrospinal fluid in multiple sclerosis. *J Clin Invest* 1998; 102: 1045–1050.
15. Hauser SL, Waubant E, Arnold DL, et al. B-cell depletion with rituximab in relapsing–remitting multiple sclerosis. *N Engl J Med* 2008; 358: 676–688.
16. Kowarik MC, Pellkofer HL, Cepok S, et al. Differential effects of fingolimod (FTY720) on immune cells in the CSF and blood of patients with MS. *Neurology* 2011; 76: 1214–1221.
17. Polman CH, Reingold SC, Banwell B, et al. Diagnostic criteria for multiple sclerosis: 2010 revisions to the McDonald criteria. *Ann Neurol* 2011; 69: 292–302.
18. Takahashi T, Fujihara K, Nakashima I, et al. Establishment of a new sensitive assay for anti-human aquaporin-4 antibody in neuromyelitis optica. *Tohoku J Exp Med* 2006; 210: 307–313.
19. Chihara N, Aranami T, Sato W, et al. Interleukin 6 signaling promotes anti-aquaporin 4 autoantibody production from plasmablasts in neuromyelitis optica. *Proc Natl Acad Sci USA* 2011; 108: 3701–3706.
20. Gohda M, Kunisawa J, Miura F, et al. Sphingosine 1-phosphate regulates the egress of IgA plasmablasts from Peyer's patches for intestinal IgA responses. *J Immunol* 2008; 180: 5335–5343.
21. Kabashima K, Haynes NM, Xu Y, et al. Plasma cell S1P1 expression determines secondary lymphoid organ retention versus bone marrow tropism. *J Exp Med* 2006; 203: 2683–2690.
22. Corcione A, Casazza S, Ferretti E, et al. Recapitulation of B-cell differentiation in the central nervous system of patients with multiple sclerosis. *Proc Natl Acad Sci USA* 2004; 101: 11064–11069.
23. Harp CT, Ireland S, Davis LS, et al. Memory B cells from a subset of treatment-naive relapsing–remitting multiple sclerosis patients elicit CD4(+) T-cell proliferation and IFN-gamma production in response to myelin basic protein and myelin oligodendrocyte glycoprotein. *Eur J Immunol* 2010; 40: 2942–2956.
24. Ruffin N, Lantto R, Pensieroso S, et al. Immune activation and increased IL-21R expression are associated with the loss of memory B cells during HIV-1 infection. *J Intern Med* 2012; 272: 492–503.
25. Gerdes J, Lemke H, Baisch H, et al. Cell cycle analysis of a cell proliferation-associated human nuclear antigen defined by the monoclonal antibody Ki-67. *J Immunol* 1984; 133: 1710–1715.
26. Odendahl M, Mei H, Hoyer BF, et al. Generation of migratory antigen-specific plasma blasts and mobilization of resident plasma cells in a secondary immune response. *Blood* 2005; 105: 1614–1621.
27. Chihara N, Aranami T, Oki S, et al. Plasmablasts as migratory IgG-producing cells in the pathogenesis of neuromyelitis optica. *PLoS One* 2013; 8: e83036.
28. Budde K, L Schmouder R Nashan B, et al. Pharmacodynamics of single doses of the novel immunosuppressant FTY720 in stable renal transplant patients. *Am J Transpl* 2003; 3: 846–854.
29. Vaessen LM, Van Besouw NM, Mol WM, et al. FTY720 treatment of kidney transplant patients: A differential effect on B cells, naive T cells, memory T cells and NK cells. *Transpl Immunol* 2006; 15: 281–288.
30. Mehling M, Brinkmann V, Antel J, et al. FTY720 therapy exerts differential effects on T-cell subsets in multiple sclerosis. *Neurology* 2008; 71: 1261–1267.
31. Johnson TA, Lapierre Y, Bar-Or A, et al. Distinct properties of circulating CD8+ T cells in FTY720-treated patients with multiple sclerosis. *Arch Neurol* 2010; 67: 1449–1455.
32. Johnson TA, Evans BL, Durafourt BA, et al. Reduction of the peripheral blood CD56(bright) NK lymphocyte subset in FTY720-treated multiple sclerosis patients. *J Immunol* 2011; 187: 570–579.
33. Nylander A and Hafler DA. Multiple sclerosis. *J Clin Invest* 2012; 122: 1180–1188.
34. Meinl E, Krumbholz M and Hohlfeld R. B-lineage cells in the inflammatory central nervous system environment: Migration, maintenance, local antibody production and therapeutic modulation. *Ann Neurol* 2006; 59: 880–892.
35. Von Budingen HC, Bar-Or A and Zamvil SS. B cells in multiple sclerosis: Connecting the dots. *Curr Opin Immunol* 2011; 23: 713–720.